

# The spheroidization of fibrous, eutectic composites at high temperatures

D. R. H. JONES

*Department of Metallurgy and Materials Science, University of Cambridge, UK*

An analysis is made of experimental data on the high-temperature spheroidization of Fe, Cu<sub>2</sub>S and Cu<sub>2</sub>O rods in the FeS—Fe, Cu—Cu<sub>2</sub>S and Cu—Cu<sub>2</sub>O eutectics. The work indicated that breakdown in FeS—Fe took place by diffusion in either the matrix or in the rod-matrix boundary. In contrast, spheroidization in Cu—Cu<sub>2</sub>S probably depended on transport in either the rod or the interphase boundary, and in Cu—Cu<sub>2</sub>O breakdown took place by diffusion in the eutectic rods only. The latter results confirm that the diffusivities of atomic species in eutectic matrices are not necessarily good guides for predicting the high-temperature stabilities of fibrous, eutectic composites.

## 1. Introduction

In an effort to produce composite materials able to withstand high temperatures, much attention has been devoted to determining the thermal stability of aligned, fibrous, eutectic composites [1-8]. In addition, several theoretical models have been developed to explain the geometrical changes induced in eutectic rods by capillarity [5, 9-13]. However, few attempts have been made to obtain information on the precise mechanisms of instability by making quantitative analyses of the existing data. In the present paper, the theory of eutectic spheroidization is, with appropriate extensions, used to analyse some of the most interesting results available (for the FeS—Fe [3], Cu—Cu<sub>2</sub>S [4] and Cu—Cu<sub>2</sub>O [4] rod-like eutectics) with a view to identifying the rate-controlling process.

## 2. Preliminary considerations

At elevated temperatures, the eutectic rods in the present systems develop periodic variations in radius of the form shown in Fig. 1. These variations become more pronounced with time so that, eventually, each rod breaks up into a row of equidistant spheres of equal radii. The experimental data enable approximate values to be derived for the parameters (defined in Fig. 1) of  $r_0$ ,  $s$ ,  $\lambda(\max)$ , and  $\dot{r}(z=0, \Delta r \sim r_0/2)$ .

The observed spheroidization may be controlled by diffusion in either the matrix, the rod, or the rod-matrix boundary. If interfacial kinetics are ignored, diffusion in either the rod

or the boundary may be shown theoretically to lead to a value for  $\lambda(\max)$  of  $9r_0$  [10]. Alternatively, if diffusion in the matrix is rate-controlling,  $\lambda(\max)$  should be  $14r_0$  for the present values of  $s/r_0$  ( $\sim 6$ ) [11]. If interfacial kinetics are significant,  $\lambda(\max)$  is predicted to be appreciably larger than these values (see Appendix 1). Clearly, because of the degrees of freedom involved, the rate-controlling process cannot easily be deduced by comparing experimental and theoretical  $\lambda(\max)$  values.

Fortunately, however, the controlling diffusional mechanism may in principle be distinguished by (a) computing from the present data approximate diffusivities for the three possible diffusion paths, and (b) comparing these diffusivities with independent values for the rod and matrix phases, and typical values for interphase boundaries. Accordingly, the following section is devoted to summarizing and, where necessary, deriving approximate formulae for this purpose.

## 3. Evaluation of diffusion coefficients

### 3.1. Diffusivities in the interphase boundary

Consider the case where interfacial kinetics may be ignored, the effect of mechanical stress may be neglected (see Appendix 2), and the limiting process is the diffusion of component 1 in the rod-matrix boundary. Then, after Nichols and Mullins [10],

$$D_{11} \sim \frac{\lambda^2(\max) \dot{r} RT}{8C_{11} \bar{V}^2 \gamma} \cdot \frac{r_0}{\delta}, \quad (1)$$

with symbols given by:  $D_{1i}$ , interfacial diffusivity of component 1;  $R$ , gas constant;  $T$ , absolute temperature;  $C_{1i}$ , interfacial concentration of mobile atoms of component 1;  $\bar{V}$ , molar volume of rod phase;  $\gamma$ , interphase boundary energy;  $\delta$ , width of boundary.

### 3.2. Diffusivities in the rod phase

In a similar manner we may write, after [10],

$$D_{1(\text{rod})} \sim \frac{\lambda^2 (\text{max}) \dot{r} RT}{4C_{1(\text{rod})} \bar{V}^2 \gamma} \quad (2)$$

### 3.3. Diffusivities in the matrix phase

The case of diffusion in the matrix for  $\Delta r \sim r_0/2$  is not analogous to the situations treated by Nichols and Mullins [10] and Cline [11] and must therefore be treated in more detail. More specifically, phase differences between the shape variations of adjacent rods lead to a more complex type of mass transport between rods than considered previously [11]. It is relatively simple to show that the flux  $j_{1(\text{matrix})}$  to any protrusion on a given rod from one of the six nearest neighbouring rods is defined by

$$0 \lesssim j_{1(\text{matrix})} \lesssim D_{1(\text{matrix})} C_{1(\text{matrix})} \frac{(\gamma \bar{V}/r_0)/RT(s - 2r_0)}{\quad} \quad (3)$$

In this expression the upper and lower limits to  $j_{1(\text{matrix})}$  correspond respectively to a shape variation of a neighbouring rod which is exactly out of, or in, phase with that of the central rod. Now the mean area sustaining  $j_{1(\text{matrix})}$  is nearly  $\pi s \lambda(\text{max})/12$ , or  $15r_0^2$ . Thus the total flow to a protrusion on the given rod from the neighbouring rods,  $\dot{m}_1$ , is the sum of six terms each equal to  $15r_0^2 j_{1(\text{matrix})}$ . On average, half of the adjacent rods will have shape variations exactly out of phase with that of the central rod, and half in phase. Thus

$$\dot{m}_1 \sim 3 \times 15r_0^2 \cdot D_{1(\text{matrix})} C_{1(\text{matrix})} \frac{(\gamma \bar{V}/r_0)}{RT(s - 2r_0)} \quad (4)$$

The flux from A to B on the central rod,  $J_{1(\text{matrix})}$ , is given by the upper limit to  $j_{1(\text{matrix})}$  in Equation 4 because the path length for diffusion from A to B through the matrix, roughly  $\frac{1}{2}\lambda(\text{max})$ , approximates here to  $(s - 2r_0)$ . Since the mean area sustaining  $J_{1(\text{matrix})}$  is nearly  $\pi(s/2 - r_0)^2$ , or  $13r_0^2$ , the total flow towards B from the two adjacent intrusions,  $\dot{M}_1$ , is  $13r_0^2 \cdot 2J_{1(\text{matrix})}$ . Hence

$$\dot{M}_1 \sim 26r_0^2 D_{1(\text{matrix})} C_{1(\text{matrix})} \frac{(\gamma \bar{V}/r_0)}{RT(s - 2r_0)} \quad (5)$$

By combining Equations 4 and 5 with the relation  $\pi r_0 \lambda(\text{max}) \dot{r}/\bar{V} \sim \dot{m}_1 + \dot{M}_1$  we have finally

$$D_{1(\text{matrix})} \sim \frac{\lambda^2 (\text{max}) \dot{r} RT}{45C_{1(\text{matrix})} \bar{V}^2 \gamma} \quad (6)$$

TABLE I Minimum diffusion coefficients for the Cu—Cu<sub>2</sub>S, Cu—Cu<sub>2</sub>O and FeS—Fe eutectics calculated from spheroidization data.

System	$D_{1i}$ (mm <sup>2</sup> sec <sup>-1</sup> )	$D_{1(\text{rod})}$ (mm <sup>2</sup> sec <sup>-1</sup> )	$D_{1(\text{matrix})}$ (mm <sup>2</sup> sec <sup>-1</sup> )
Cu—Cu <sub>2</sub> S*	1 1 = Cu, S	10 <sup>-3</sup> 1 = Cu, S	10 <sup>-4</sup> , 1 = Cu 1, 1 = S†
Cu—Cu <sub>2</sub> O*	10 <sup>2</sup> 1 = Cu, O	10 <sup>-1</sup> 1 = Cu, O	10 <sup>-2</sup> , 1 = Cu 10 <sup>2</sup> , 1 = O†
FeS—Fe‡	10 <sup>-3</sup> 1 = Fe, S	10 <sup>-6</sup> , 1 = Fe 10 <sup>-2</sup> , 1 = S†	10 <sup>-7</sup> 1 = Fe, S

\*At 1 to 5K below the eutectic temperature [4].

† $C_1 \sim 0.01$  mol %;  $C_1 \sim 50$  mol % in all other cases.

‡At 13K below the eutectic temperature [3].

## 4. Discussion

Table I lists values of  $D_{1i}$ ,  $D_{1(\text{rod})}$  and  $D_{1(\text{matrix})}$  calculated with Equations 1, 2 and 6 from the experimental data of Tables I and II and Fig. 1. Since both interfacial kinetics and the transport of other species may have partly controlled spheroidization, these diffusivities are minima.

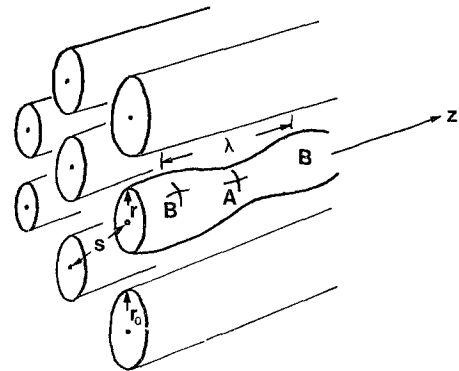


Figure 1 Schematic illustration of the spheroidization of an eutectic rod in the FeS—Fe, Cu—Cu<sub>2</sub>S and Cu—Cu<sub>2</sub>O systems. The rod has shape  $r \sim r_0 + \Delta r \cos 2\pi z/\lambda(\text{max})$ .  $\lambda(\text{max})$  is found, from optical micrographs [3, 4], to be  $(10 \pm 5)r_0$ .

Taking first the present values of  $D_{1i}$ , that obtained for FeS—Fe agrees well with those determined for interphase boundaries at high

TABLE II Approximate values of the physical constants used for calculating the diffusion coefficients listed in Table I.

System	$r_0$ ( $\mu\text{m}$ )	$\delta$ (nm)	$\gamma$ ( $\text{mJ m}^{-2}$ )	$\dot{r}$	$\bar{V}$ ( $\text{ml mol}^{-1}$ )
Cu—Cu <sub>2</sub> S	0.4 [4]	0.3	500 [4]	$0.1 \mu\text{m sec}^{-1}$ [4] 10	
Cu—Cu <sub>2</sub> O	0.7 [4]	0.3	15 [4]	$0.1 \mu\text{m sec}^{-1}$ [4] 10	
FeS—Fe	1.5 [3]	0.3	500 [3]	$10 \text{ pm sec}^{-1}$ [3] 10	

temperatures [14]. In contrast, the values tabulated for Cu—Cu<sub>2</sub>S and Cu—Cu<sub>2</sub>O are intolerably large. In this connection the copper-based systems were held at temperatures so high (see Table I) that  $\delta$  may have been up to 100 times the value assumed herein, due both to interfacial melting [15] and to the presence of molten, segregated impurity at the interphase boundaries. This being the case, the values of  $D_{11}$  for Cu—Cu<sub>2</sub>S and Cu—Cu<sub>2</sub>O should be reduced respectively to  $10^{-2}$  and  $1 \text{ mm}^2 \text{ sec}^{-1}$ . The former figure is almost the same, within error, as a typical self diffusion coefficient for a liquid metal near the melting point ( $\sim 10^{-3} \text{ mm}^2 \text{ sec}^{-1}$ ) [16]; but the value for Cu—Cu<sub>2</sub>O is still too large to be admissible.

 TABLE III Independent values for diffusivities in the rod and matrix phases of the Cu—Cu<sub>2</sub>S, Cu—Cu<sub>2</sub>O and FeS—Fe eutectics.

System	$D_{1(\text{rod})}$ ( $\text{mm}^2 \text{ sec}^{-1}$ )	$D_{1(\text{matrix})}$ ( $\text{mm}^2 \text{ sec}^{-1}$ )
Cu—Cu <sub>2</sub> S	$\sim 1$ $1 = \text{Cu}$ [17a, b]	$10^{-6}$ , $1 = \text{Cu}$ [16] $\sim 10^{-4}$ , $1 = \text{S}$ [18]
Cu—Cu <sub>2</sub> O	$\sim 10^{-2}$ [17c]	$10^{-6}$ , $1 = \text{Cu}$ [16] $10^{-3}$ , $1 = \text{O}$ [19]
FeS—Fe	$10^{-10}$ , $1 = \text{Fe}$ [16] $10^{-7}$ , $1 = \text{S}$ [16]	$10^{-2}$ , $1 = \text{Fe}$ [20] $\sim 10^{-6}$ , $1 = \text{S}$ [17d]

Turning to the present values of  $D_{1(\text{matrix})}$  and  $D_{1(\text{rod})}$ , it is interesting to compare these with the appropriate diffusivities determined at the same temperatures and compositions by independent methods (see Tables I and III). Taking first the FeS—Fe system, the directly derived coefficients of diffusion in the rod phase are far too small to permit the mass transfer required during spheroidization. The present values for  $D_{1(\text{matrix})}$  are, however, comparable to, or less than, the appropriate published values. These facts, taken together with the reasonable

value obtained for  $D_{11}$ , indicate that spheroidization in FeS—Fe takes place by diffusion in either the matrix or the rod-matrix boundary.

In the case of Cu—Cu<sub>2</sub>S and Cu—Cu<sub>2</sub>O, the published values for the matrix diffusivities (Table III) are, with one possible exception, not nearly large enough to provide the required mass transport. Unfortunately the independent experimental data for diffusion in Cu<sub>2</sub>S and Cu<sub>2</sub>O do not appear to be complete (see Table III); but the available information, considered in the light of the revised values of  $D_{11}$ , indicates that (a) spheroidization in Cu—Cu<sub>2</sub>S probably occurs by diffusion in either the rod or the rod-matrix boundary, (b) spheroidization in Cu—Cu<sub>2</sub>O occurs by transport in the rods themselves.

In conclusion the above type of approach is in principle applicable to a variety of eutectic and other systems; and further work in this area should be of interest.

## Appendix 1

The effect of interfacial kinetics on

$\lambda(\text{max})/r_0$

For  $\Delta r \ll r_0$ , the difference in interfacial curvature between A and B is  $2[(1/r_0^2) - (4\pi^2/\lambda^2)]\Delta r$  [11]. Thus, from capillarity theory,

$$|\Delta\mu_1| = 2\gamma\bar{V}(1/r_0^2 - 4\pi^2/\lambda^2)\Delta r,$$

where  $\Delta\mu_1$  is the difference in chemical potential of component 1 at A and B. Clearly, if spheroidization is controlled by interfacial kinetics, the rate of the process will be greatest when terms  $|\Delta\mu|$  are maximized, or when  $\lambda$  is infinite. Thus interfacial kinetics make  $\lambda(\text{max})/r_0$  larger than when diffusion is the only significant process.

## Appendix 2

The effect of mechanical stresses

In general, composites are in a state of stress due to differential contractions of the phases during the thermal history of the system. Fortunately, in Cu—Cu<sub>2</sub>S and Cu—Cu<sub>2</sub>O spheroidization took place a short distance

behind the growth front during directional solidification of the alloy; thus, from the temperature differences given in Table I, the differential contraction of rods and matrices should have been only 0.001%, resulting in a negligible state of stress.

In contrast, the specimens of FeS—Fe were cooled to room temperature after growth, resulting in a strain of roughly 1% which may well have led to significant plastic flow. Thus, on reheating the alloy to the temperature of spheroidization, plastic flow may well have occurred in the opposite sense. In this connection the yield stresses of metals at temperatures near the melting point, although much less than at room temperature, are nevertheless not negligible [21]; in fact they are comparable to typical values of  $\gamma/r_0$ . Unfortunately, since the detailed calculation of the stress components would prove exceedingly difficult, it does not seem possible to specify the error resulting from the neglect of mechanical stresses in FeS—Fe. It would, therefore, be worthwhile to study the spheroidization of this system by a technique equivalent to that used for the other alloys.

### Acknowledgements

The author is grateful to Professor R. W. K. Honeycombe for providing research facilities. He is also indebted to the Science Research Council for their financial support, and to the Master and Fellows of Christ's College, Cambridge, for help in the form of a Fellowship.

### References

1. B. J. BAYLES, J. A. FORD and M. J. SALKIND, *Trans. Met. Soc. AIME* **239** (1967) 844.
2. A. R. T. DESILVA and G. A. CHADWICK, *Metal Sci. J.* **6** (1972) 157.
3. S. MARICH, *Met. Trans.* **1** (1970) 2953.
4. S. MARICH and D. JAFFREY, *ibid* **2** (1971) 2681.
5. H. B. SMARTT, L. K. TU and T. H. COURTNEY, *ibid* **2** (1971) 2717.
6. Y. G. NAKAGAWA and G. C. WEATHERLY, *Acta Met.* **20** (1972) 345.
7. H. B. SMARTT and T. H. COURTNEY, *Metal. Trans.* **4** (1973) 217.
8. J. L. WALTER and H. E. CLINE, *ibid* **4** (1973) 33.
9. F. A. NICHOLS and W. W. MULLINS, *J. Appl. Phys.* **36** (1965) 1826.
10. *Idem*, *Trans. Met. Soc. AIME* **233** (1965) 1840.
11. H. E. CLINE, *Acta Met.* **19** (1971) 481.
12. G. C. WEATHERLY and Y. G. NAKAGAWA, *Scripta Met.* **5** (1971) 777.
13. A. J. ARDELL, *Met. Trans.* **3** (1972) 1395.
14. A. D. BRAILSFORD and H. B. AARON, *J. Appl. Phys.* **40** (1969) 1702.
15. W. A. MILLER and G. A. CHADWICK, *Acta Met.* **15** (1967) 607.
16. C. J. SMITHELLS, "Metals Reference Book" (Butterworths, London, 1967) pp. 644, 645, 666, 683.
17. *Diffusion Data*, (a) **4** (1970) 134; (b) **4** (1970) 476; (c) **4** (1970) 100; (d) **3** (1969) 78.
18. F. MOYA and F. CABANE-BROUTY, *Compt. Rend. Acad. Sci. Paris, Ser. C* **264** (1967) 1543.
19. R. L. PASTOREK and R. A. RAPP, *Trans. Met. Soc. AIME* **245** (1969) 1711.
20. E. T. TURKDOGAN, *ibid* **242** (1968) 1665.
21. J. H. WESTBROOK, *Trans. ASM* **45** (1953) 221.

Received 21 August and accepted 26 November 1973.